

Shot peening using spherical micro specimens generated in high-throughput processes

Strahlen mittels sphärischer Mikroproben aus Hochdurchsatzprozessen

J. Kämmler¹, N. Wielki^{1,2}, N. Guba^{1,2}, N. Ellendt², D. Meyer^{1,2}

Mechanical surface treatment processes like shot peening induce plastic deformation in the near surface areas of the peened workpiece leading to changes in surface and subsurface properties, e.g. hardness alteration and generation of compressive residual stress. While changes of the processed part are desired because of the lifetime extending influence, changes of the shot material are normally neglected as it is chosen to be highly resistant. Within this work plastic deformation of the shot material X210Cr12 and AlSi12 is examined. By investigating the plastic deformation of the particles, an indirect analysis of material properties, e.g. the yield stress or the hardness, is possible. A consideration of the particle velocities also enables conclusions about the materials properties. Those properties are conventionally obtained in a material, time, and cost intensive way. Using the same jet pressure, the investigations show lower velocities and less pronounced plastic deformation for the X210Cr12 specimens. Due to their higher mass, the X210Cr12 particles of same diameter are accelerated slower and therefore reach a lower impact velocity compared to AlSi12 particles. Furthermore, the lower plastic deformation at identical velocities can be explained with the higher yield stress of the X210Cr12 particles.

Keywords: Micro specimens / impulse atomization / single droplet generation / particle characterization / shot peening / plastic deformation

Mechanische Verfahren zur Oberflächenbearbeitung, wie beispielsweise Kugelstrahlen, erzeugen plastische Deformationen in oberflächennahen Bereichen des Strahlguts. Diese führen zu Veränderungen der Randzoneneigenschaften, wie beispielsweise der Härte, und zur Ausbildung von Druckeigenspannungen. Während diese Änderungen des Strahlguts aufgrund ihrer lebensdauererlängernden Wirkung erwünscht sind, wird die Veränderung des Strahlmittels in der Regel vernachlässigt, da für dieses ein widerstandsfähiges Material verwendet wird. Im Rahmen dieser Arbeit wird die plastische Deformation der Strahlmittel aus X210Cr12 sowie AlSi12 untersucht. Durch die Analyse der Partikeldeformation wird eine indirekte Beschreibung von Materialeigenschaften, wie beispielsweise der Streckgrenze oder der Härte, ermöglicht. Die Betrachtung der Partikelgeschwindigkeiten lässt ebenfalls Rückschlüsse auf die Materialeigenschaften zu, welche konventionell in material-, zeit- und kostenintensiven Versuchen ermittelt werden. Wird derselbe

¹ Leibniz Institute for Materials Engineering IWT, Badgasteiner Straße 3, 28359 Bremen, Germany

² University of Bremen and MAPEX Center for Materials and Processes, Bibliothekstraße 1, 28359 Bremen, Germany

Corresponding author: N. Wielki, Leibniz Institute for Materials Engineering IWT, Badgasteiner Straße 3, 28359 Bremen, Germany, E-Mail: wielki@iwt.uni-bremen.de

Strahlendruck verwendet, zeigen die Untersuchungen der X210Cr12 Partikel geringere Geschwindigkeiten sowie weniger stark ausgeprägte Deformationen. Aufgrund der höheren Masse werden die X210Cr12 Partikel desselben Durchmessers bei gleichem Druck weniger stark beschleunigt, wodurch im Vergleich zu den AlSi12 Partikeln geringere Aufprallgeschwindigkeiten folgen. Weiterhin kann die geringere plastische Deformation bei, über eine Variation des Druckes erreichten, identischen Geschwindigkeiten unter anderem auf die höhere Streckgrenze von X210Cr12 zurückgeführt werden.

Schlüsselwörter: Mikroproben / Impulserstäubung / Einzeltropfenerzeugung / Partikelcharakterisierung / Kugelstrahlen / plastische Deformation

1 Introduction and motivation

To meet the requirements of industries such as the automotive and aerospace industry, finishing processes as for example shot peening are used to increase durability of highly stressed parts. Thereby it is possible to improve the fatigue performance by projecting small, hard particles at high velocity onto a metallic part which introduces compressive residual stresses and strain hardening [1,2]. Besides improved strength properties these industries also demand further development of lightweight materials to reduce weight [3,4]. Furthermore, the process optimisation requires new materials which are able to speed up production processes in order to save costs [3]. Regarding the behaviour of different materials in various applications, increasing demands require a fast development and characterization of new materials. Because of the need to characterize new materials, their development is determined by the testing methods which are standardized for macroscopic specimens. Consequently, developing new materials is material, time, and cost intensive which is why another approach is desirable [5,6]. To reduce required raw materials and supplies, a synthesis and characterization of smaller specimens is favourable. As the investigation of thin films (below 100 nm), which is already possible, neglects the influence of the microstructure, a bulk properties based approach is required [5]. Although conventional material characterization (e.g. tensile test) might not be performed on such samples, information about the material behaviour can still be obtained. For example, plastic deformation due to mechanical impact is related to the materials strength properties (e.g. yield stress). The principle of hardness measurement already uses this inter-

relation [7,8]. The geometrical quantity obtained from the indentation changes according to the properties of the tested material. For a constant test load, deeper and larger indentations are obtained for materials with a lower yield stress [8]. Since a lower force is necessary to induce plastic deformation, the dependency between the deformation and the yield stress enables its indirect analysis. Considering this interrelation, further analysis might reveal mathematical correlations to support material choice. In order to obtain statistically reliable results and to generate specimens with varied and defined composition in a short time, processes with high production rates of small specimens such as droplet processes could be taken into account. While gas atomization techniques aim at the production of small particles (< 100 μm), much larger and spherical particles (300 μm -2000 μm) can be produced by single fluid atomization techniques such as impulse atomization or single droplet generation [9–11]. These particles develop because of the melts surface tension. They are characterized by a large volume-related surface. Typical application areas for atomization are technical operations such as surface coating or production of metallic powders, where the quality or fineness of the spray is of high importance [12,13]. Since the drop on demand technique produces molten metal droplets, it is of great interest in research laboratories or in industrial applications such as 3D printing [14,15]. Obtained cooling rates are still high enough to allow rapid solidification, so that a fine, equiaxed microstructure can be obtained [16]. Since the sample size becomes large compared to its microstructural features it is possible to conclude to bulk properties. As rapid solidification techniques, both processes show a deviation from the equilibrium which causes

different solidification conditions and enables the creation of supersaturated microstructures [17]. Depending on the falling distance, the droplet size as well as on other parameters, a homogeneous microstructure can be achieved [11]. Although favourable specimen properties are expected using the processes described above, an investigation of the material properties following conventional testing procedures is not possible because of the specimen size. Consequently, a new method needs to be established. Since an interrelation between plastic deformation and materials properties exists, processes with a mechanical main effect, as for example deep rolling, hammering or shot peening can be considered [18]. As the latter is a process where spherical particles are accelerated by e. g. a gas flow to interact with the surface of the contact plate, a similar acceleration of the micro specimens could be used to induce plastic deformation [19]. The kinetic energy of the particles and thereby their velocity depends on the acceleration, flow conditions, and the mass of the particles, i. e. the particle diameter and the density. During the conventional process, the kinetic energy is converted into forming energy and the contact plate is plastically deformed by the impact. Hence, compressive residual stresses develop and the hardness of the workpiece increases due to strain hardening [20]. While the deformation of the mechanically impacted surface is favourable, the properties of the particles are normally chosen in a way to ensure that they do not deform plastically. Therefore, their hardness should be at least as high as the hardness of the contact plate [19]. If the former is considerably smaller than the latter, the conversion of the kinetic particle energy into forming energy is expected to result in a deformation of the particles as the effect of the process on the contact plate decreases. This normally not intended deformation of the particles might be used to characterize the e. g. mechanical behaviour of the small specimens mentioned above. Therefore, easily determinable characteristic values, so called “descriptors”, which vary depending on the material and the microstructure are utilized instead of conventional material properties, which cannot be accessed using micro-specimens. Although a correlation of the determined “descriptors” with individual material properties would be desirable, it is likely that the change of their values depends on various factors. Within the scope of SFB 1232, a mathematical cor-

relation based on optimization functions is to be carried out following the determination of the “descriptors”. In the present study, the properties of spherical specimens generated by impulse atomization and in a process of single droplet generation are investigated regarding their velocity before impact and their plastic deformation after a shot peening process. These values are then qualitatively put into relation with material properties as described above, *Figure 1*.

2 Generation and characterization of micro specimens

2.1 Generation of micro specimens

To highlight the differences of the investigation, AlSi12 and X210Cr12 specimens are utilized within this work because of their considerably different properties. For synthesis of AlSi12 particles, aluminium (purity: 99.99 %) and silicon (purity: 99.99 %) were melted in an Al₂O₃ crucible using an induction furnace in a nitrogen atmosphere. After holding the melt at 690 °C (melt superheat: 100 K) for 15 minutes to achieve homogenization, droplets were produced using the impulse atomization process through 89 orifices (diameter 500 µm) [9]. While falling free in a nitrogen atmosphere, the particles solidified and were collected after a falling distance of 4.5 m. To synthesize X210Cr12 particles, a com-

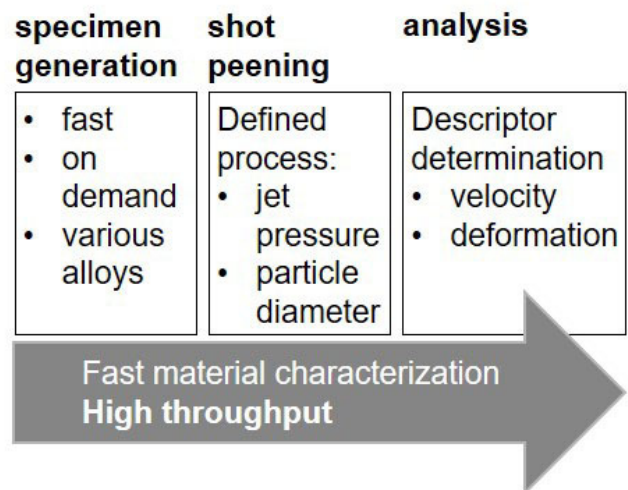


Figure 1. Visualization of the approach.

Bild 1. Visualisierung des Vorgehens.

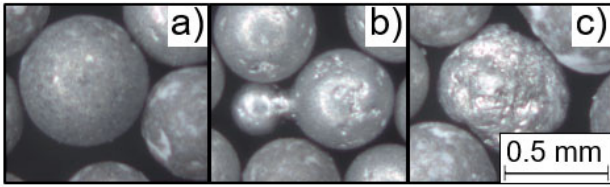


Figure 2. Comparison of different AlSi12 particle forms (a) as intended, b) aggregates, c) rough, not perfectly spherical particles.

Bild 2. Vergleich verschiedener AlSi12 Partikelformen (a) wie beabsichtigt, b) Aggregate, c) raue, nicht perfekt sphärische Partikel.

mercial alloy was inductively melted in an argon atmosphere in an Al_2O_3 crucible to a temperature of 1475 °C. This time, the particles were generated using a pneumatic high temperature drop-on-demand generator [11]. The particles were quenched after a falling distance of 810 mm in oil to maintain the as-solidified microstructure.

2.2 Characterization of micro specimens

To separate particles of different diameters, all specimens are sieved before the shot peening process. Particles are characterized before and after the process to identify the plastic deformation by the measurement of the geometrical changes. As defects and deviations from the spherical lead to unpredictable flight behaviour and determined deformations cannot be traced back to the mechanical impact, spherical specimens with a smooth surface are favourable.

2.2.1 Particle size and geometry classification

Size and shape of the specimens were measured using the incident light microscope Leica DVM2500 (Leica Microsystems) equipped with the digital camera DVM2500 and objective nosepiece VZ700 C. The images were analysed using the software LAS V4.6 which enables the determination of the particle diameter as well as the examination of plastic deformation due to the shot peening process. Since the latter value can only be measured when it is visible under the microscope, particles need to be

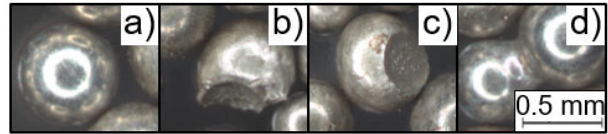


Figure 3. Comparison of different X210Cr12 particle forms (a) as intended, b) particles with pits, c) particles with a flattening, d) aggregates.

Bild 3. Vergleich verschiedener X210Cr12 Partikelformen (a) wie beabsichtigt, b) Partikel mit Ausbrüchen, c) Partikel mit Abplattungen, d) Aggregate.

orientated. Similar to the measurement, this is performed manually. The available AlSi12 specimens were divided into four particle classes ($d_1 = 0.45 \text{ mm}-0.50 \text{ mm}$, $d_2 = 0.50 \text{ mm}-0.60 \text{ mm}$, $d_3 = 0.60 \text{ mm}-0.71 \text{ mm}$, $d_4 = 0.71 \text{ mm}-0.80 \text{ mm}$). Besides the intended spherical shape, the particles can show deviations from this geometry. There are aggregates or non-spherical particles, *Figure 2*. Furthermore, some particles had a very rough surface with cracks.

Analysis of generated particles revealed, that the deviations from the spherical shape increased with increasing particle diameter. The X210Cr12 specimens generated with the drop on demand technique showed diameters varying between 500 μm -800 μm . Their reflective surface is less rough compared to the AlSi12 particles. Specimens of this material also deviated from the intended spherical shape, *Figure 3*. Besides aggregates, pits and plastic deformations can occur already before the shot peening process.

2.2.2 Microstructural characterization

The samples were embedded, ground and polished for microstructural characterization, *Figure 4*. The microstructure of the aluminium particle on the left side, belonging to the diameter group 450 μm -500 μm , shows aluminium areas (white) next to the AlSi-eutectic (grey) and the large silicon crystals (reflective, silver). Further, pits near or with connection to the surface are visible. The microstructure of the X210Cr12 reveals differences between the near-surface area and the core of the particle, *Figure 4b*. While the structure in the core contains branched dendrites, the subsurface area ex-

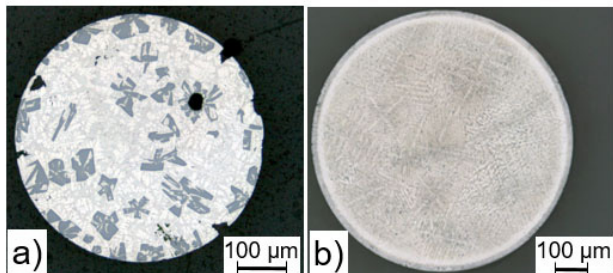


Figure 4. Microstructure of a) AlSi12 and b) X210Cr12 particles.

Bild 4. Mikrostruktur von a) AlSi12 und b) X210Cr12 Partikeln.

hibits a fine acicular structure which can possibly be explained by the fast quenching in the oil filled collectors. Hardness measurements performed in the middle of the particle on the polished surfaces revealed a value of 167 ± 15 HV1 for the AlSi12 particle and a hardness of 452 ± 5 HV1 for the X210Cr12 sample.

3 Mechanical treatment of micro specimens

3.1 Shot peening

Although a conventional shot peening set-up is used, the aim of the process differs from the conventional approach. As described above, the experiments focus on the plastic deformation of the particles which is why the micro samples can be called the “workpieces” in this case. In order to avoid plastic deformation of the contact plate, hardened 100Cr6 (hardness approximately 60 HRC) is chosen as its material. The experiments are monitored by a high-speed camera (Motion Pro; from the Imaging Solutions company) which is connected to the microscope by an adapter as pictured in the experimental set-up, *Figure 5*. As presented, the nozzle is positioned on a V-Profile which is placed on a XY-Table. The contact plate is located in front of the nozzle outlet and the white background is used to increase the contrast. To realize an exposure time of $16 \mu s$, two additional light sources (of the company Dedocool) are necessary. The recording frequency was set at 32200 Hz. To start the process and the measuring, a trigger is utilized.

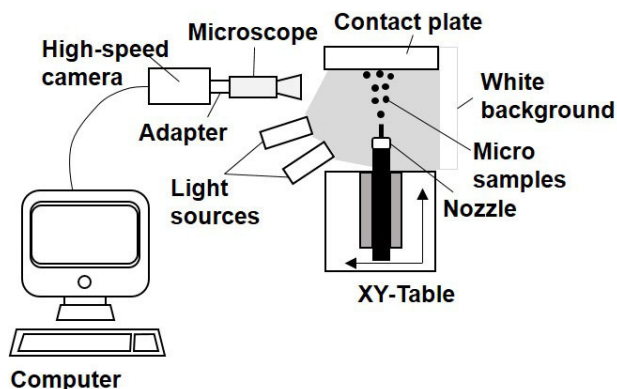


Figure 5. Schematic diagram of the experimental set-up.

Bild 5. Schematische Darstellung des experimentellen Aufbaus.

3.2 Plastic deformation

To enable conclusions about the material-property-determined forming-behaviour of the particles, the linear plastic deformation Δl due to the flattening is examined after the shot peening process. It is defined as difference between the initial particle radius r and the distance from the centre to the flattened surface after the impact, *Figure 6*. The deformation of the particle perpendicular to this direction was not part of the investigations presented here. Influenced by the jet pressure different linear plastic deformations are measured. As plotted for both investigated materials, an increased jet pressure results in an increasing linear plastic deformation, *Figure 7*. In each case the error bars picture the standard deviation of five measurements. Regardless of the material or particle diameter all graphs have in common that no plastic deformation could be observed at a

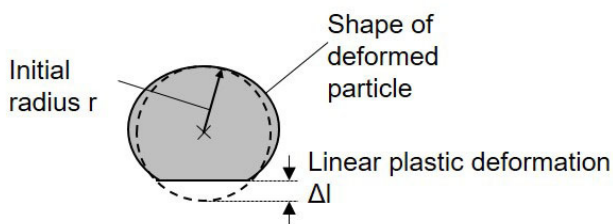


Figure 6. Schematic diagram of values analysed after the shot peening process.

Bild 6. Prinzipielle Darstellung der nach dem Strahlen an den Proben ausgewerteten Größen.

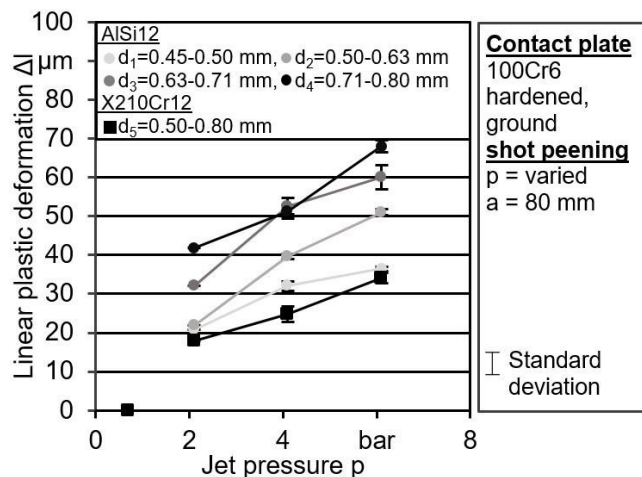


Figure 7. Development of the linear plastic deformation Δl depending on the jet pressure.

Bild 7. Änderung der Abplattungshöhe in Abhängigkeit des Strahldrucks.

jet pressure of 0.7 bar. Because of pits, which can be observed for all AISi12 graphs at a jet pressure of 4.1 bar, a linear dependence between the linear plastic deformation and the jet pressure within the range of 2.1 bar to 6.1 bar is not clearly identifiable. Only the X210Cr12 graph rises approximately linearly between 2.1 bar and 6.1 bar. For the same jet pressure, all linear plastic deformations determined for the AISi12 particles are higher than the ones determined for the X210Cr12 particles. This is due to the lower hardness obtained for the AISi12 particles which correlates with their lower yield stress, so that plastic deformation occurs at lower stresses. For both materials, the yield stress is exceeded between 0.7 bar and 2.1 bar. To estimate the development of the graphs within these two points, more pressures will be investigated. Regarding the AISi12 particles, the influence of an increasing diameter is manifested in an increase of the measured linear plastic deformation, Figure 7.

Since an influence of the shot peening process on the microstructure of the specimens is possible, a characterization of the microstructure after the process is carried out. Regarding the microstructure of the particles shot peened with a pressure of 6.1 bar plastic deformations, pits (AISi12) and cracks (X210Cr12) are visible, Figure 8. Since the dark areas visible for AISi12 also occur investigating particles previous to the peening, their origin cannot be clearly assigned to the shot peening process.

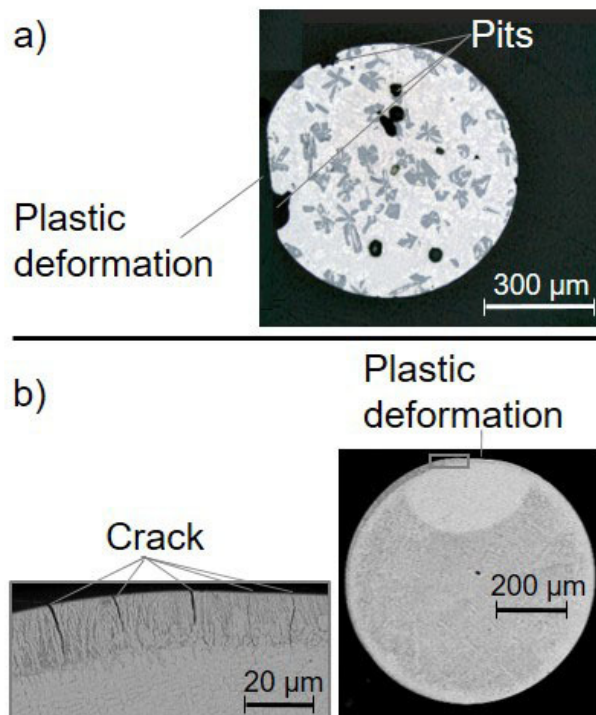


Figure 8. Microstructure of the particles after the shot peening process a) AISi12, b) X210Cr12.

Bild 8. Mikrostruktur von a) AISi12 und b) X210Cr12 Partikeln nach dem Kugelstrahlen.

Their characteristic distribution and size suggest that silicon crystals have broken out as a result of the mechanical loads during preparation of metallographic sections. The cracks visible in the X210Cr12 specimens can mainly be observed at the surface. This might be due to the brittle material behaviour as a result of the fast cooling. Since the cracks at the edges of the flattened surface are stronger pronounced than the cracks in the middle, there might be an interrelation to the degree of deformation.

Neither the pits nor the cracks can be clearly connected to the pulsed loading. The microstructure of X210Cr12 does not show any indicators for a structural transformation. Additionally with a force of 10 mN in connection with a holding time of 10 s performed microhardness measurements did not reveal new information. The indentations were placed in lines starting from the flattened side up to a depth of 250 μm .

3.3 Peening velocity

As the velocity of the particles is influenced by the jet pressure and the density of the particles, differences between the two materials are expected. To determine the particle velocity v , the high speed camera described in chapter 3.1 is utilized. Recorded pictures at different times t_1 and t_2 are taken to identify the current distances s_1 and s_2 of the particle from the nozzle. Using this distances and the corresponding time the velocity of the particle can be determined by following equation.

$$v = \frac{s_2 - s_1}{t_2 - t_1} \quad (1)$$

Velocities are calculated for particles of both materials using three different jet pressures (2.1 bar, 4.1 bar and 6.1 bar), *Figure 9*. While the AlSi12 particles have a diameter between 0.71 mm and 0.80 mm, the particle diameter of the X210Cr12 specimens varies between 0.50 mm and 0.80 mm. Within the considered jet pressure range it can be seen, that the particle velocity increases approximately linear with an increasing jet pressure. Using the same jet pressure for the AlSi12 and the X210Cr12 specimens, different velocities can be observed. As the former are expected to have a density of 2650 kg m^{-3} and the latter are expected to have a density of 7850 kg m^{-3} , the lower velocity of X210Cr12 results from higher inertia forces while

accelerating drag forces are maintained for a constant particle diameter. For a jet pressure of 4.1 bar, the X210Cr12 particles show approximate the same velocity as the AlSi12 particles with a diameter between 0.50 mm and 0.71 mm when a jet pressure of 2.1 bar is applied. As matching velocities lead to material dependent different linear plastic deformation, values determined for the AlSi12 particles tend to be higher, *Figure 10*. Regarding the particle velocity for the AlSi12 particles, an increasing particle diameter results in increasing particle velocities, *Figure 9*. This could be traced back to the mass flow [19]. As more particles of a smaller diameter, than particles of a larger diameter, pass the supply hose, a collision is more likely. By colliding, the particles lose energy and their velocity reduces. Alternatively, the higher velocity of the larger particles can be explained by the fact that the flow changes to a plug flow. Since the particles are not surrounded by the flow anymore but pushed forwards, the accelerations effectiveness increases. The increasing particle velocity with increasing diameter is more pronounced for low jet pressures. For higher jet pressures, the differences between the diameter influenced particle velocities decreases.

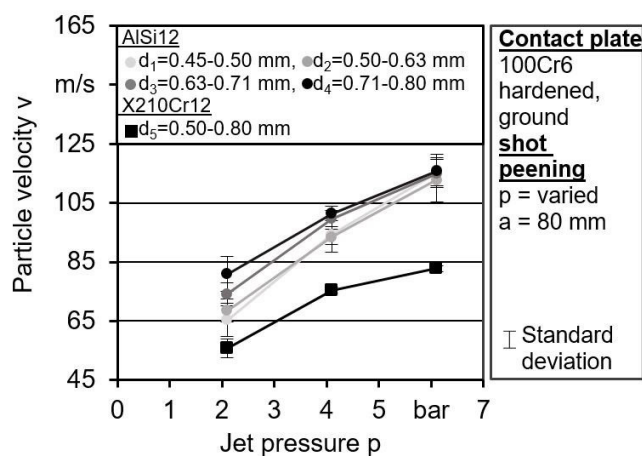


Figure 9. Determined particle velocity using different jet pressures for a constant distance $a = 80 \text{ mm}$.

Bild 9. Ermittelte Partikelgeschwindigkeiten für unterschiedliche Strahlgeschwindigkeiten bei konstantem Abstand $a = 80 \text{ mm}$ zwischen Düse und Werkstück.

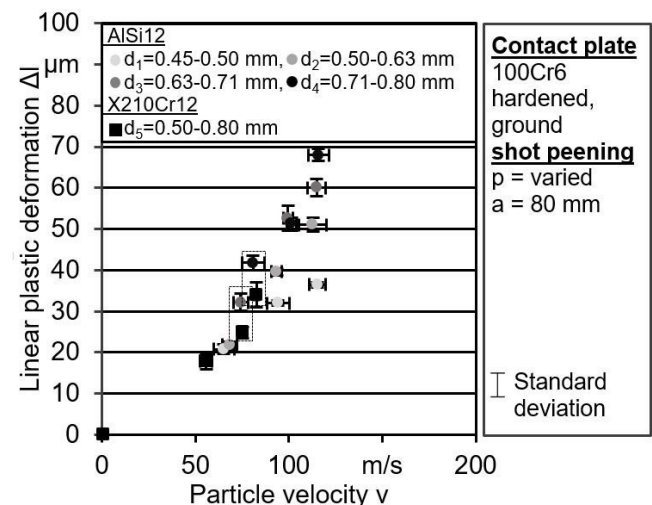


Figure 10. Interrelation of the determined linear plastic deformation Δl and the particle velocity (dashed lined box: Matching particle velocities).

Bild 10. Zusammenhang der ermittelten Abplattungshöhen sowie Partikelgeschwindigkeiten (gestrichelter Kasten: übereinstimmende Partikelgeschwindigkeiten).

4 Conclusions and outlook

The aim of this work was to investigate whether a shot peening process could be utilized to obtain a determinable plastic deformation of micro specimens which could be correlated with conventional material properties in order to quickly characterize materials. As the deformation due to the impact is connected to the material properties of the particles, the linear plastic deformation Δl resulting of the process was investigated. Since plastic deformation takes place at first when the yield stress of the material is exceeded, a plastic deformation of the specimens was first determined at jet pressures around 2 bar. A further increase of the jet pressure leads to increasing linear plastic deformation. As the X210Cr12 specimens show a higher yield stress than the aluminium particles, their plastic deformation is less pronounced and the determined linear plastic deformation is lower. Cracks and pits determined in additional investigations of the microstructure of the shot after the peening process cannot be clearly connected to the pulsed loading. Also no indicators for structural transformation of the X210Cr12 specimens can be seen. Regarding the velocity of the specimens leaving the nozzle a material independent increase can be observed as the jet pressure rises. When the same jet pressure is applied on both materials, the AlSi12 particles show a higher velocity. This can be traced back to their low mass because of their comparatively low density. Contrary to the expectations, particles with a bigger diameter and thereby a higher mass showed higher velocities than smaller particles. Possibly this can be traced back to the lower mass flow as the probability of the particles to collide decreases when less particles pass the supply hose. Alternatively, the changing flow conditions might be responsible for this effect. It can be concluded, that the method presented to investigate the properties of the shot peened particles reveals information according to the material behaviour of the specimens. Since the analysis of the deformed particles yet is done manually, further investigation could be carried out to improve the procedure. The results obtained cannot be linked to defined specimens and only give an overview. Analysing the same particle before, during and after the shot peening process could reveal further information which could possibly be linked to conventionally defined material properties as e.g. the results of a tensile test.

Acknowledgements

Financial support of the subprojects U04 ‘Mechanical Treatment’ and U01 ‘Single droplet Solidification’ of the CRC 1232 ‘Farbige Zustände’ funded by the Deutsche Forschungsgemeinschaft (DFG, German Research Foundation) – Projektnummer 276397488 – SFB 1232 is gratefully acknowledged.

5 References

- [1] T. Klotz, D. Delbergue, P. Bocher, M. Lévesque, M. Brochu, *Int. J. Fatigue* **2018**, *110*, 10.
- [2] A. Gariépy, H.Y. Miao, M. Lévesque, *Adv. Eng. Softw.* **2017**, *114*, 121.
- [3] M. Holmes, *Reinf. Plast.* **2017**, *4*, 237.
- [4] K.H. Yang, *Basic Finite Element Method as Applied to Injury Biomechanics*, Academic Press, **2017**.
- [5] L. Mädler, *Proceedings of the 4th International Conference on Nanomanufacturing*, **2014**.
- [6] N. Ellendt, L. Mädler, *HTM J. Heat Treatm. Mat.* **2018**, *73*, 1.
- [7] E. Macherauch, H.W. Zoch, *Praktikum in Werkstoffkunde*, Vieweg+Teubner Verlag / Springer Fachmedien Wiesbaden GmbH, Wiesbaden **2011**.
- [8] Y. Cao, Z. Xue, X. Chen, D. Raabe, *Scr. Mater.* **2008**, *5*, 518.
- [9] H. Henein, *Mater. Sci. Eng.* **2002**, *1*, 92.
- [10] H. Henein, V. Uhlenwinkel, U. Fritsching, *Metal Sprays and Spray Deposition*, Springer International Publishing, **2017**.
- [11] N. Ellendt, N. Ciftci, C. Goodreau, V. Uhlenwinkel, L. Mädler, *IOP Conf. Ser.: Mater. Sci. Eng.* **2016**, 12057.
- [12] M. Majumder, C. Rendall, M. Li, N. Behabtu, J.A. Eukel, R.H. Hauge, H.K. Schmidt, M. Pasquali, *Chem. Eng. Sci.* **2010**, *6*, 2000.
- [13] P. Deepu, C. Peng, S. Moghaddam, *Exp. Therm. Fluid Sci.* **2018**, *92*, 243.
- [14] A. Amirzadeh, M. Raessi, S. Chandra, *Exp. Therm. Fluid Sci.* **2013**, *47*, 26.

- [15] T.M. Lee, T.G. Kang, J.S. Yang, J. Jo, K.Y. Kim, B.O. Choi, D.S. Kim, *IEEE Trans. Electron. Packag. Manuf.* **2008**, 3, 202.
- [16] P.S. Grant, *Prog. Mater. Sci.* **1995**, 4, 497.
- [17] Y. Xu, N. Ellendt, X.G. Li, V. Uhlenwinkel, U. Fritsching, *Trans. Nonferrous Met. Soc. China* **2017**, 7, 1636.
- [18] E. Brinksmeier, M. Garbrecht, D. Meyer, *CIRP Ann.* **2008**, 1, 541.
- [19] V. Schulze, *Modern Mechanical Surface Treatment*. Wiley-VCH, Weinheim, **2006**.
- [20] B. Scholtes, O. Vöhringer, *Materialwiss. Werkstofftech.* **1993**, 12, 421.

Received in final form: October 16th 2018